INDIAN INSTITUTE OF TECHNOLOGY HYDERABAD

DEPARTMENT OF PHYSICS

Rotation Curve Modelling to constrain Dynamical Mass Distribution in Spirals

Author:
Ambica Govind

Supervisors:
Dr Paolo Salucci
Dr Shantanu Desai

December 2024

Abstract

This study aims to find the dark matter fraction in a sample of 1357 galaxies from the PROBES Dataset by modelling their Rotation Curves. In order to get rid of errors caused due to systematics and non-circularities we bin the data radially and in velocity space and stack them to generate a set of 8 synthetic rotation curves. To model them we take a top-down approach by decomposing the RC into disk and Dark Matter halo(Burkert and NFW) contributions and fit the RCs via an MCMC Code. We get closed contours and convergence in our MCMC results, successfully modelling the RCs

Acknowledgments

I am grateful to Dr. Paolo Salucci and Dr. Gauri Sharma for graciously providing me with the opportunity to work on this subject. Their mentorship and expertise have been invaluable throughout this journey.
I am indebted to Dr. Shantanu Desai for his guidance, support, and uplifting encouragement. His mentorship has taught me much more than just astrophysics.
I thank Dr. Sandeep Haridasu and Dr. Paolo Salucci for providing me with the data samples and helping me figure out why the fitting wouldn't give the expected results.
Furthermore, I am immensely thankful to my parents for their support and unwavering belief in me at every stage of my career.

Contents

Chapter 1

Introduction

1.1 Mass Discrepancies

Mass Discrepancies in the universe are ubiquitous, arising from observations of galactic and extragalactic systems as well as from predictions of General Relativity. They are a subject of active research and debate in the cosmology community. Two schools of thought attempt to explain them: The Standard Model of Cosmology(ΛCDM), that invokes non-luminous, undetected form of mass in the universe called dark matter, and Modified Gravity Theories, that attempt to modify existing laws of gravity to explain these discrepancies instead of resorting to unseen mass.
What follows is a brief review of historical evidences pointing at mass discrepancies at various astronomical scales.

Oort in 1932 found a discrepancy of $0.052 M_{\odot} pc^{-3}$ in the mean mass density of the galactic disk at the solar radius based on vertical motions of stars. He found that the luminous mass was insufficient to provide the restoring force to sustain the observed stellar oscillations. The discrepancy was attributed to fainter stars, meteors and nebular material. With time discoveries of fainter stars were made, supplemented by that of neutral hydrogen from the 21-cm line as well as molecular hydrogen. The gap thus closed in to about $0.008 M_{\odot} pc^{-3}$, which was still unaccounted for (1).

Zwicky (2) measured the apparent velocity dispersion of galaxies in the Coma Cluster to be about 1000 km/s. The velocity dispersion inferred by applying Virial Theorem to the luminous mass was in fact 80 km/s, meaning that they were moving too fast to remain gravitationally bound to the cluster. This indicated the presence of an additional 'unseen mass' component(dark matter) responsible for this inconsistency. However back then it was not known that majority of the cluster mass resides in the diffuse intracluster medium so the discrepancy was exaggerated considerably. Current cluster observations map X-Ray emission from the ICM to determine temperature and density profiles, after which the equation of hydrostatic equilibrium can be used to calculate the cluster mass. Now the discrepancy stands at a factor of $\approx$ 8(3).

A major development occurred when rotation curves(RCs) of spiral galaxies were found to asymptotically become flat as opposed to the Keplerian $\frac{1}{\sqrt{r}}$ fall-off using optical photometry (4), spectroscopy (5) and the more robust 21-cm observations (6). Note that these observations were also taken at the largest radii observable, where the $\frac{1}{\sqrt{r}}$ behaviour *should* have been observed. Yet again, dark matter was necessitated. The constancy of the rotation curve after a certain radius suggests a mass density profile resembling $\rho \propto r^{-2}$.

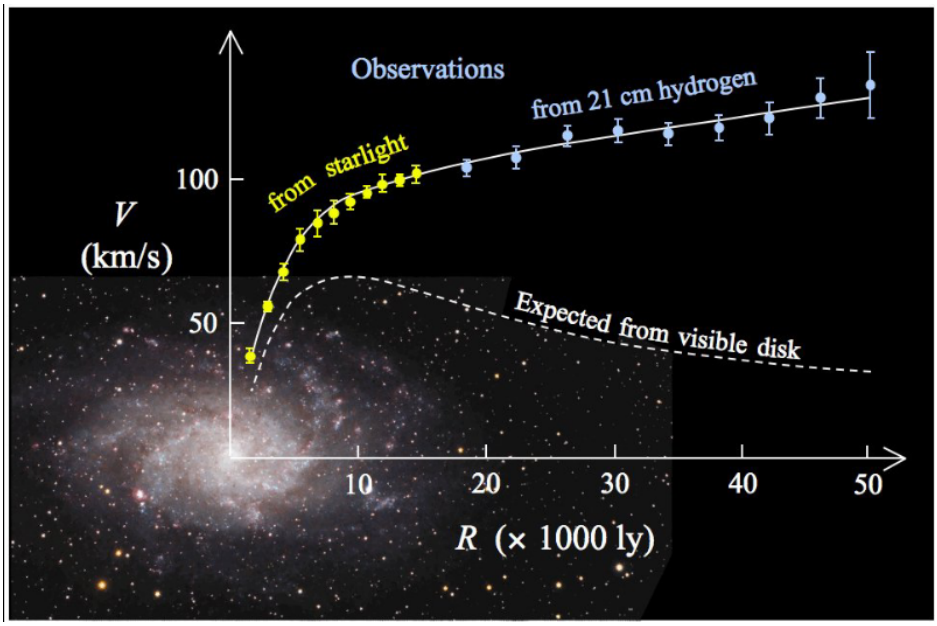

Figure 1.1: M33 Galaxy and its rotation curve (7)

Yet another piece of evidence is found in the Local Group. One would think that Milky Way and Andromeda were, at some point, moving away from each other due to Hubble Expansion, however now it is known that their collision is imminent. This change in momentum requires an $\frac{M}{L} > 80$ along the line of sight, much greater than the $\frac{M}{L}$ of stars alone, which is on an average of the order of $1\frac{M_\odot}{L_\odot}$.

There is also an abundance of cosmological evidence supporting the existence of dark matter. Latest measurements of cosmological parameters from Planck(8) determine the mean cosmological matter density parameter to be $\Omega_m = 0.315 \pm 0.007$ using measurements of Cosmic Microwave Background(CMB) Polarization, temperature and lensing. But measurements of Big Bang Nucleosynthesis place the baryonic matter density $\Omega_b \approx 0.02$(9). The same is confirmed in Planck 2018 results. This is hard evidence for Dark Matter, non-baryonic at that.

Finally the existence of dark matter as a part of the Concordance Model *a priori* predicts several other observational results relative heights of peaks in the CMB Power Spectrum(10), gravitational lensing(11), and the formation of large scale

structure(12). ΛCDM now attests that the energy budget of the universe dominated by dark energy(70%)followed by dark matter($25 - 30\%$), with ordinary baryonic matter amounting to only 5% (12). In this framework, Dark Matter is understood to be cold and collisionless, only form of interaction with ordinary matter being gravity.

Dark Matter, however, is not a solution to all problems in astrophysics. There exist a bunch of unpredicted observations and unobserved predictions(13) mostly manifesting as fine-tuning problems in the cosmological parameters and baryonic feedback. Some of the unpredicted observations are,in fact, elegant consequences of Modified Gravity Theories. In addition, dark matter particles have eluded discovery through both direct(at the Large Hadron Collider) and indirect methods for detection(based on WIMP self-annihilation products)(14),(15). Furthermore, its particle nature has not been pinned down yet.

This project explores the efficacy of the dark matter formulation in explaining galactic dynamics. This has been done numerous times earlier, here we explore the same with new observations of rotation curves. The theory, methodology and dataset are described in the following sections and chapters.

1.2 Dark Matter in Galaxies

The necessity of dark matter in galaxies first came in because of the problem of disk instability in spirals. Stars in spiral galaxies were known to be dynamically cold(i.e. low velocity dispersion) which created problems of disk instability, as per simulations(16). The problem could be solved by embedding the galaxy in a spherical dark matter halo, the first appearance in (16).

The presence of dark matter in galaxies is evident from RCs. In highly luminous galaxies baryons dominate close to the centre; dark matter dominates progressively away from it whereas in LSB(Low Surface Brightness Galaxies) dark matter dominates throughout the galaxy (17). The gravitational potential of the spiral can be decomposed into components as follows:

$$\phi = \phi_D + \phi_b + \phi_{DM} + \phi_{H_2} + \phi_{HI}$$

corresponding to the disk, bulge, dark matter halo, molecular and atomic hydrogen respectively. This can be related to the circular velocity:

$$V_c^2 = r\frac{d\phi}{dr} = V_D^2 + V_b^2 + V_{DM}^2 + V_{H_2}^2 + V_{HI}^2$$

The Poisson Equation relates the surface/spatial densities to their corresponding potentials, thus there exist four separate equations for each component:

$$\nabla^2\phi_i = 4\pi G\rho_i$$

This is the reason rotation curves are used as a proxy for gravitational potential and are thus helpful for determining the mass distribution of galaxies. As a first approximation, we only consider the disk and DM Halo components.

1.2.1 Freeman's Disk Model

de Vaucouleurs showed that surface brightness distributions of all disklike galaxies can be modelled as an inner spheroidal component and an outer exponential disk(18). The surface densities too are well described by the Exponential Thin Disk Model(19):

$$\Sigma_d(R) = \frac{M_D}{2\pi R_D^2} e^{-\frac{R}{R_D}}$$

where M_D is the mass of the disk and R_D the scale length. This density distribution translates to a circular velocity contribution like so:

$$V_D^2(R) = \frac{1}{2}\frac{GM_D}{R_D}\frac{R^2}{R_D^2}[I_0K_0 - I_1K_1] \tag{1.1}$$

I_n, K_n are Modified Bessel Functions evaluated at $0.5\frac{R}{R_D}$ for stars.

1.2.2 The Dark Matter Halo

Modern galaxy formation models propose the formation of a dark matter halo by collisionless collapse, followed by the accumulation of baryons into the centres of these potential wells accompanied by heating to virial temperature. The baryons then cool by radiating energy and shedding angular momentum leading to the formation of galaxies and in extreme enough cases, supermassive black holes(12).

The exact structure and distribution of dark matter in these halos is still a subject of debate(the core-cusp problem).
The rotation velocities in the inner regions of the disk increase linearly; this solid-body behaviour can be indicative of a core, with a large constant density in the inner parts. However N-body simulations of ΛCDM state otherwise, describing the distribution as a steep power law- a cusp with a slope $d\ln\rho/d\ln r = -1$(20).
Note that the latest simulations point towards an Einasto Profile(21) with $d\ln\rho/d\ln r = -1/n$, with n slightly varying with halo mass. Fitting Einasto profiles to RCs(22), however, leads to values of n much smaller than simulated values, essentially taking us back a full circle.As of now, there exists no credible solution to the core-cusp problem within ΛCDM.

In this project we fit the data to two most-well known models that emulate the core(the Burkert Profile(23)) and the cusp(the Navarro-Frenk-White Profile(20)).

Burkert Halo

A Burkert Halo is given by the following density profile:

$$\rho(r) = \frac{\rho_0 r_c^3}{(r + r_c)(r + r_c^2)} \tag{1.2}$$

where ρ_0 is the central density and r_c is the core radius. This expression, upon integrating gives the mass in radius r:

$$M(<r) = 2\pi\rho_0 r_c^3 \left[\ln\left(1+\frac{r}{r_c}\right) - \arctan\left(\frac{r}{r_c}\right) + \frac{1}{2}\ln\left(1+\left(\frac{r}{r_c}\right)^2\right)\right] \tag{1.3}$$

We calculate $V_{DM}^2(r)$ as $\frac{GM(<r)}{r}$

NFW Halo

An NFW Halo is given by the following density profile:

$$\rho(r) = \frac{\rho_0}{\frac{r}{r_c}\left(1+\left(\frac{r}{r_c}\right)^2\right)} \tag{1.4}$$

where ρ_0, r_c are the characteristic density and radius. Upon integrating we get the mass in radius r:

$$M(<r) = 4\pi\rho_0 r_c^3 \left[\ln\left(1+\frac{r}{r_c}\right) - \frac{r}{r+r_c}\right] \tag{1.5}$$

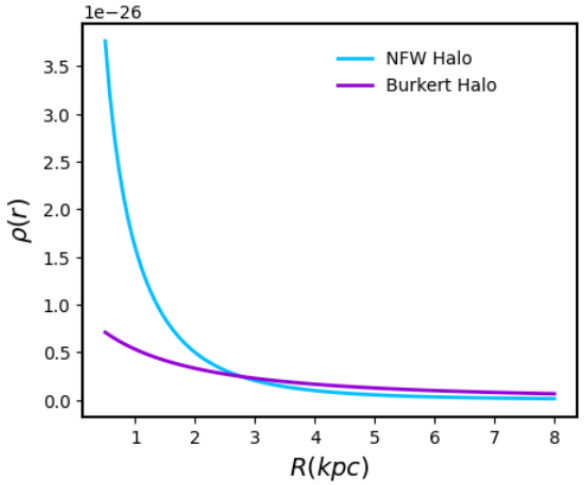

Figure 1.2: Density profiles of NFW and Burkert Halos

The dark matter fraction as a function of r, $f_{DM}(r)$, can be estimated as V_{DM}^2/V^2. The next section dwells on the objectives of this project.

1.3 Objective

The objective of this study is to model the mass distribution in a sample of 258 spiral galaxies using their galaxy rotation curves and find the dark matter fraction.

1.4 Acronyms

- R_D: Semi-major axis of the galactic disk
- R_{opt}: Optical radius, defined as the radius(on the major axis) encompassing 80% of the integrated light; $R_{opt} \approx 3R_D$
- V_{opt}: Optical velocity, the velocity at R_{opt}

Chapter 2

Data

The PROBES(Photometry & Rotation Curve Observations from Extragalactic Surveys) Catalog (24) provides extended rotation curves for 3163 late type spirals leveraging $H\alpha$ long slit spectra and HI velocity maps to provide deep spatially resolved kinematic information on these galaxies. These curves typically extend out to a deeper median extent of twice the effective half-light radius($2R_e$) or the isophotal radius $R_{23.5}$, in contrast to previous surveys such as CALIFA or MaNGA whose depth is about $1.5R_e$. The depth will help efficiently probe the flatter region of a galaxy disk beyond the transition from baryon- to dark matter-dominated systems.

No selection criteria is used in order to keep the sample complete. However only 'good' RCs that do not have spurious values of systematic velocities are selected. This leaves us with 1675 galaxies in total. Preparation involves symmetrization of RCs, after which R_{opt} is selected from the existing catalog and the corresponding V_{opt} is estimated from the velocities provided for all fiducial radii. In cases where data for V_{opt} is not available, it is set to be equal to the velocity at the furthest point of the disk for which data is there.
Further, we select a random sample of 258 galaxies from 1675 and implement all tests on this subsample. The dataset thus includes galaxy names, optical radii and velocities, absolute magnitudes and distances. Each galaxy has a RC with errors on $V(R)$.

Chapter 3

Data Analysis

The first step in preprocessing is to homogeneize the errors on $V(R)$, so that if $\Delta V(R) < 0.02V(R)$, we assign $\Delta V(R) = 0.02V(R)$. We do this so as to exclude bogus fits.
Data Analysis is done in two steps:

1. Coadding the RCs
2. Model Fitting

3.1 Coadding RCs

Individual RCs are affected by non-axisymmetric disturbances and systematics, even if relatively minor. To average these out we bin the RCs in V_{opt} to achieve a compromise between the number of data in each bin and the number of bins.

V_{opt} bin	$V_{opt}(km/s)$ range	N Galaxies	$\langle V_{opt} \rangle$	$< R_{opt} >$
1	14.16 - 75.76	32	53.11	9.99
2	76.24 - 91.36	32	82.97	7.04
3	92.79 - 106.50	32	99.75	9.31
4	106.73 - 125.49	32	115.85	11.02
5	125.58 - 139.93	32	133.26	10.04
6	140.21 - 167.96	32	153.62	11.01
7	168.23 - 193.11	32	179.67	12.87
8	193.56 - 369.37	34	240.85	15.33

An essential part of this procedure is to make the galaxies in each bin as similar as possible, only then does it make sense to average out the properties. To do this we double-normalize the RCs, transforming R vs $V(R)$ of each galaxy to its corresponding R/R_{opt} and $V(R/R_{opt})$. We further wish to analyze only the inner portion of the RC where $R/R_{opt} < 1.2$.
The final double-normalized RCs in each bin are shown below: The next step is to perform radial binning. Owing to the large difference in data density in the inner part of the RCs as opposed to the outer part, we bin radially so as to get a reasonably

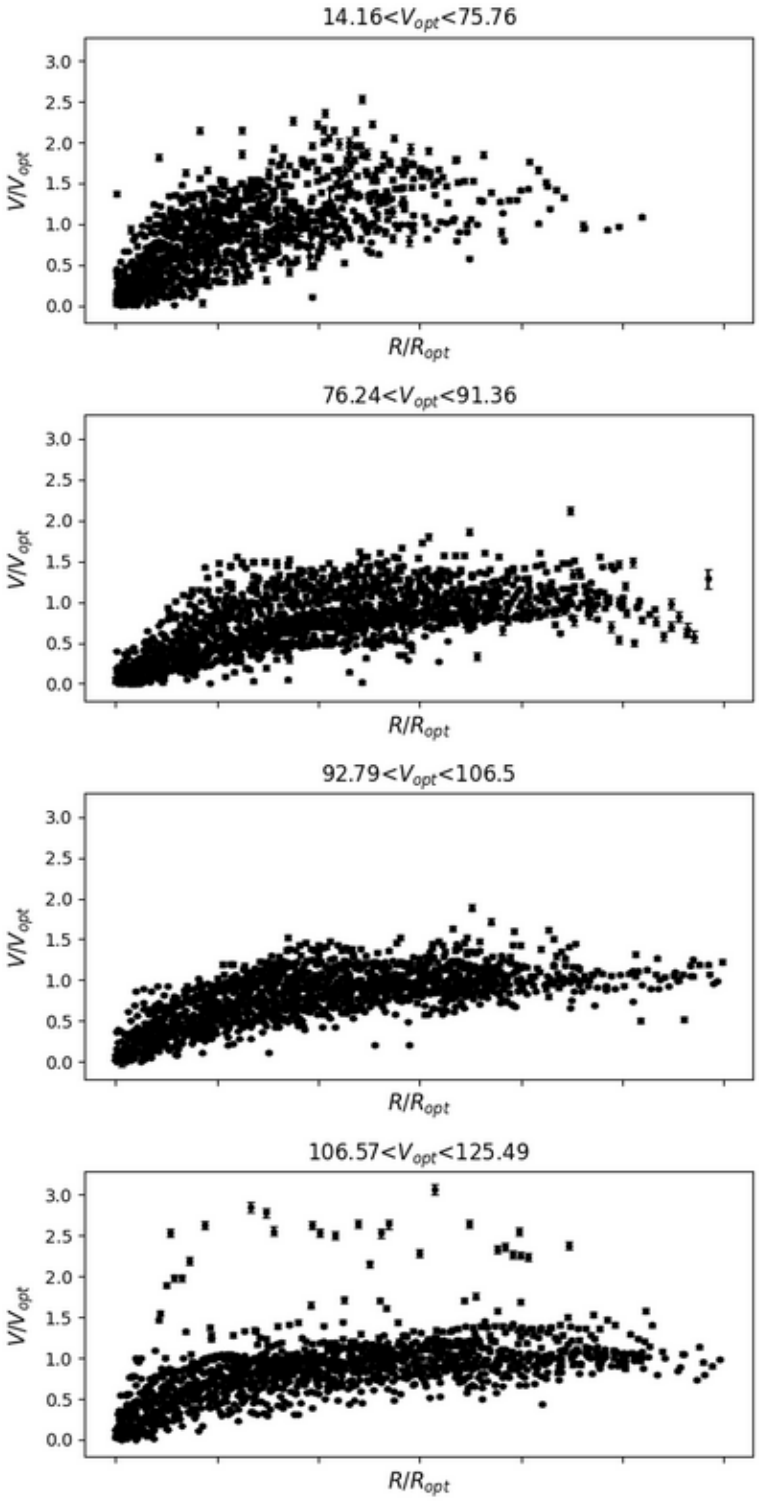
14.16<V_{opt}<75.76
76.24<V_{opt}<91.36
92.79<V_{opt}<106.5
106.57<V_{opt}<125.49
V/V_{opt}
R/R_{opt}
0.0
0.5
1.0
1.5
2.0
2.5
3.0

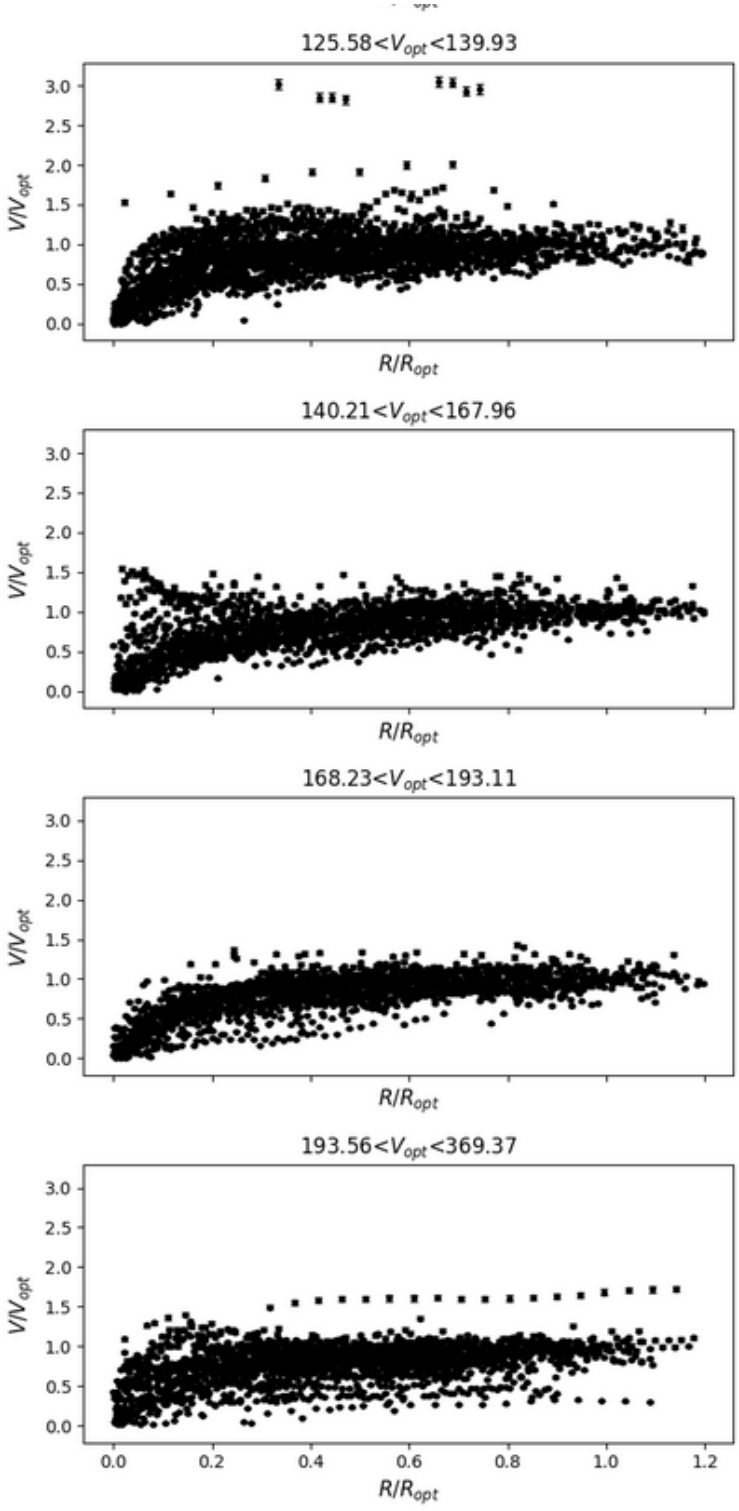
125.58<V_{opt}<139.93
140.21<V_{opt}<167.96
168.23<V_{opt}<193.11
193.56<V_{opt}<369.37
V/V_{opt}
R/R_{opt}
0.0
0.5
1.0
1.5
2.0
2.5
3.0
0.2
0.4
0.6
0.8
1.2

similar number of data points within each radial bin, alongwith a reasonable number of bins. Assuming that the ith bin has N_i datapoints, the velocity in each bin is estimated as the mean, $V_i = \frac{\Sigma_{j=1}^{N} {}^{i} v_{ij}}{N_i}$. The standard error on mean we use is:

$$\delta V_i = \sqrt{\frac{\Sigma_1^N {}_i (v_{ij} - V_i)^2}{N_i(N_i - 1)}}$$

.
The RCs are then denormalized to physical units by multiplying them by the average $\langle R_{opt} \rangle$ and $\langle V_{opt} \rangle$ in each bin. The synthetic RCs are shown below.

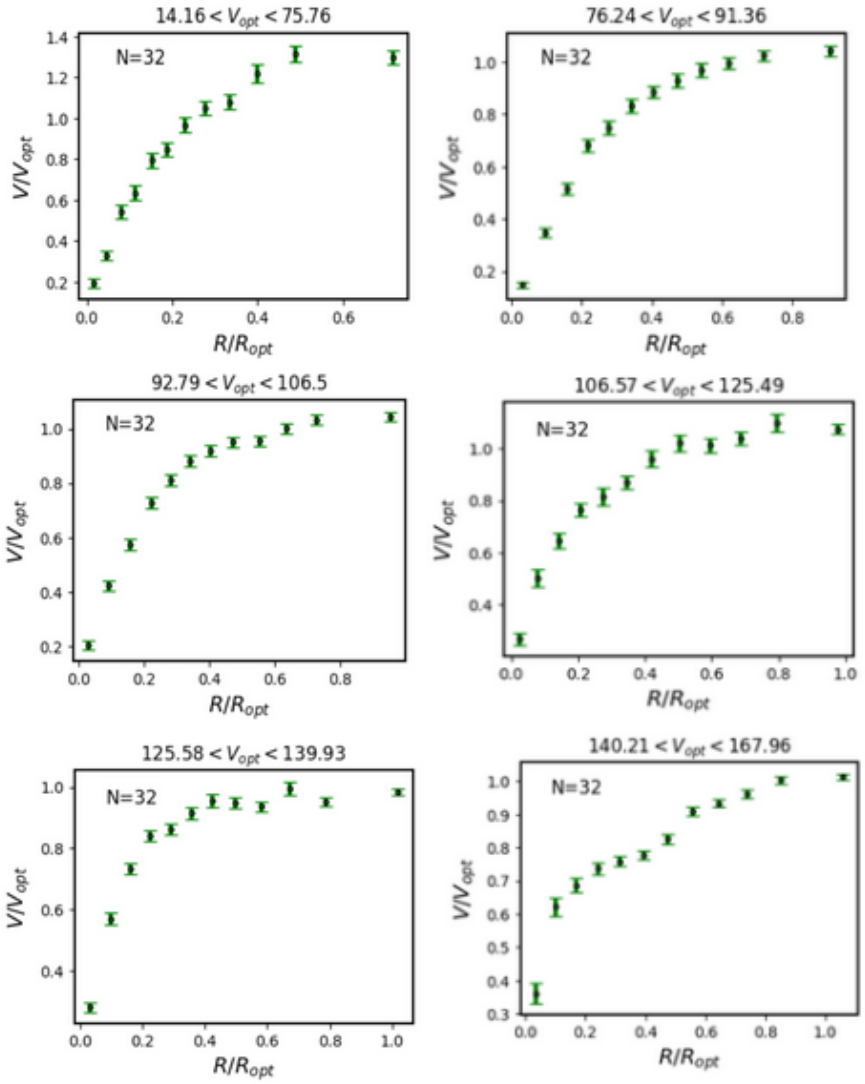

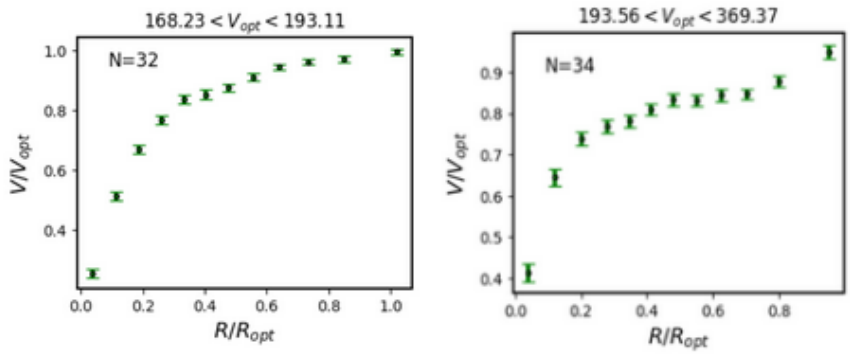

Figure 3.1: Coadded synthetic RCs in 8 bins

This method thus helps in getting rid of non-circularities and observational errors in the RCs. Note the difference in the profiles of RCs of different optical velocity ranges.

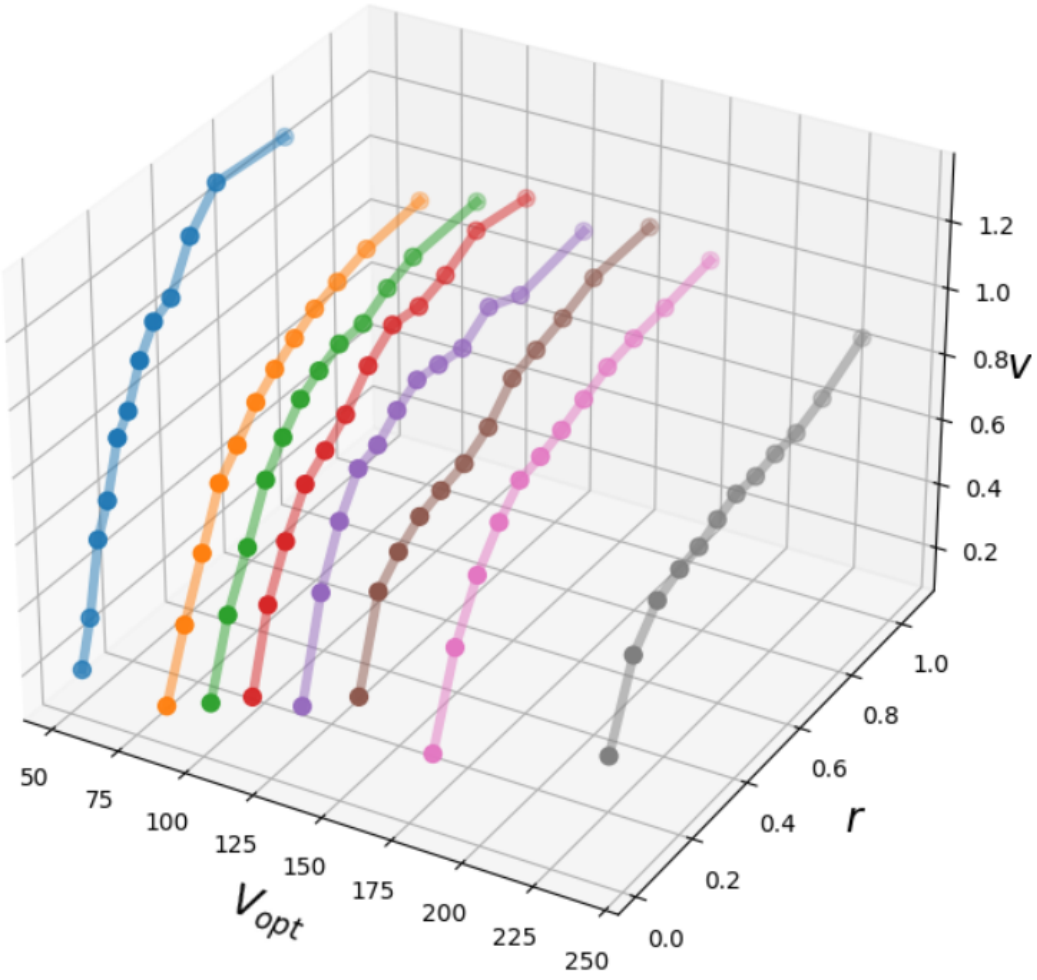

Figure 3.2: Spacing of RCs in V_{opt} space

3.2 Mass Modelling

As a first approximation to the mass model we fit the RCs only to profiles of a disk-halo combination so that:

$$V(R)^2 = V_{DM}^2 + V_D^2$$

THe disk is modelled as an exponential profile whose V_D^2 is obtained from Eq (1.1). V_{DM}^2 is calculated for both Burkert and NFW Profiles. We fit $V(R)$ to a three-parameter model characterized by the disk mass M_D, density scale ρ_o and halo scale radius R_c via a Markov Chain Monte-Carlo(MCMC) procedure. A model RC is shown below:

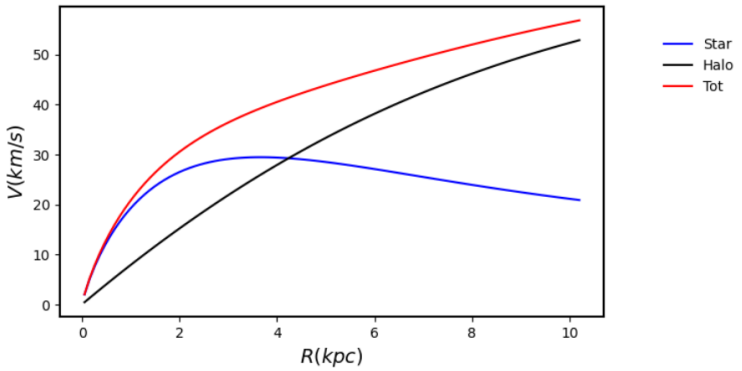

3.2.1 MCMC

MCMC is a widely used technique for Bayesian Parameter Estimation. It is a technique for sampling from a probability distribution and using those samples to approximate a desired quantity.

The cornerstone of Bayesian Techniques in statistics is the Bayes' Theorem:

$$P(M, \boldsymbol{\theta}|D) = \frac{P(D|M, \boldsymbol{\theta})P(M, \boldsymbol{\theta})}{P(D)} \tag{3.1}$$

$P(M, \theta|D)$ is the probability of a model with a parameter vector $\boldsymbol{\theta}$ being correct, called the posterior, $L = P(D|M, \theta)$ the likelihood, $P = P(M, \theta)$ the prior(quantifying any presumptions one might have regarding the model parameters) and $P(D)$ the evidence. The goal of a Bayesian Parameter Estimation algorithm is to maximize the likelihood times the prior.

MCMC is a derivative of the broader Metropolis-Hastings Algorithm. It works as follows:

1. Start from a random point θ_0 in the initial range of parameters provided, with associated posterior probability $P(\theta_0|D)$
2. Consider another point in the proposal distribution and calculate the posterior at this point $P(\theta_2|D)$

3. Move to θ_2 with aprobability $min(\frac{P(\theta_2|D)}{P(\theta_0|D)}, 1)$

4. Generate a uniform random number u from the uniform distribution [0,1) and accept the candidate sample if $u < \alpha$.

5. Repeat steps 2 through 4 until the user-specified steps are exhausted. Intuitively, the algorithm eventually lands on the $\boldsymbol{\theta}$ with highest posterior probability.

3.2.2 Fitting

The MCMC Analysis is performed through the `emcee` package in Python(25), an affine invariant sampler. Slightly differing from a traditional M-H Algorithm, it uses a series of walkers with very less correlation length to sample the parameter space effectively.

For our analysis we use informative flat priors for $\log M_D$ from 7.9 to 11.69, $\log R_C$ from 0 to 100 and $\log \rho_0$ from -18 to -25.3 . We allow 25 walkers to evolve over 5000 steps and discard the first 1000 steps for burn-in. The results follow in the next section

Chapter 4

Results

The following two pages demonstrate the MCMC fits for both kinds of halo. It appears that none of the fits are particularly good. We notice two key problems:

1. The model RCs are much higher than the data
2. In some cases the disk counterintuitively dominates outer dynamics as opposed to dark matter

To solve the problem we changed the number of bins and binning technique(whether to prioritize the uniformity of number of galaxies in each bin, or uniform binning in V_{opt}), and tweaked MCMC priors to a reasonable extent. We also tried to estimate the best fit parameters by taking the mean of the sampled parameter space, the median and even the set which gave the maximum posterior probability. However the fits were still below par.
We realized that the problem is within the data itself. The values of R_D in the

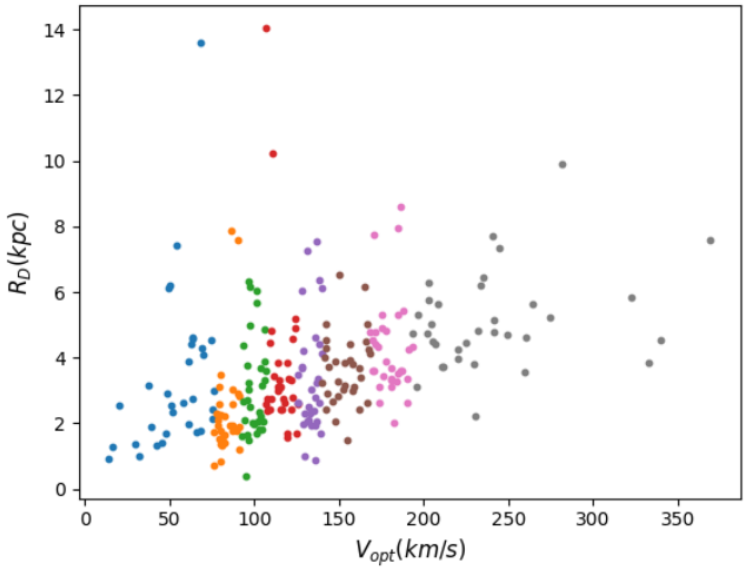

Figure 4.1: Bin-wise distribution of R_D in the subsample

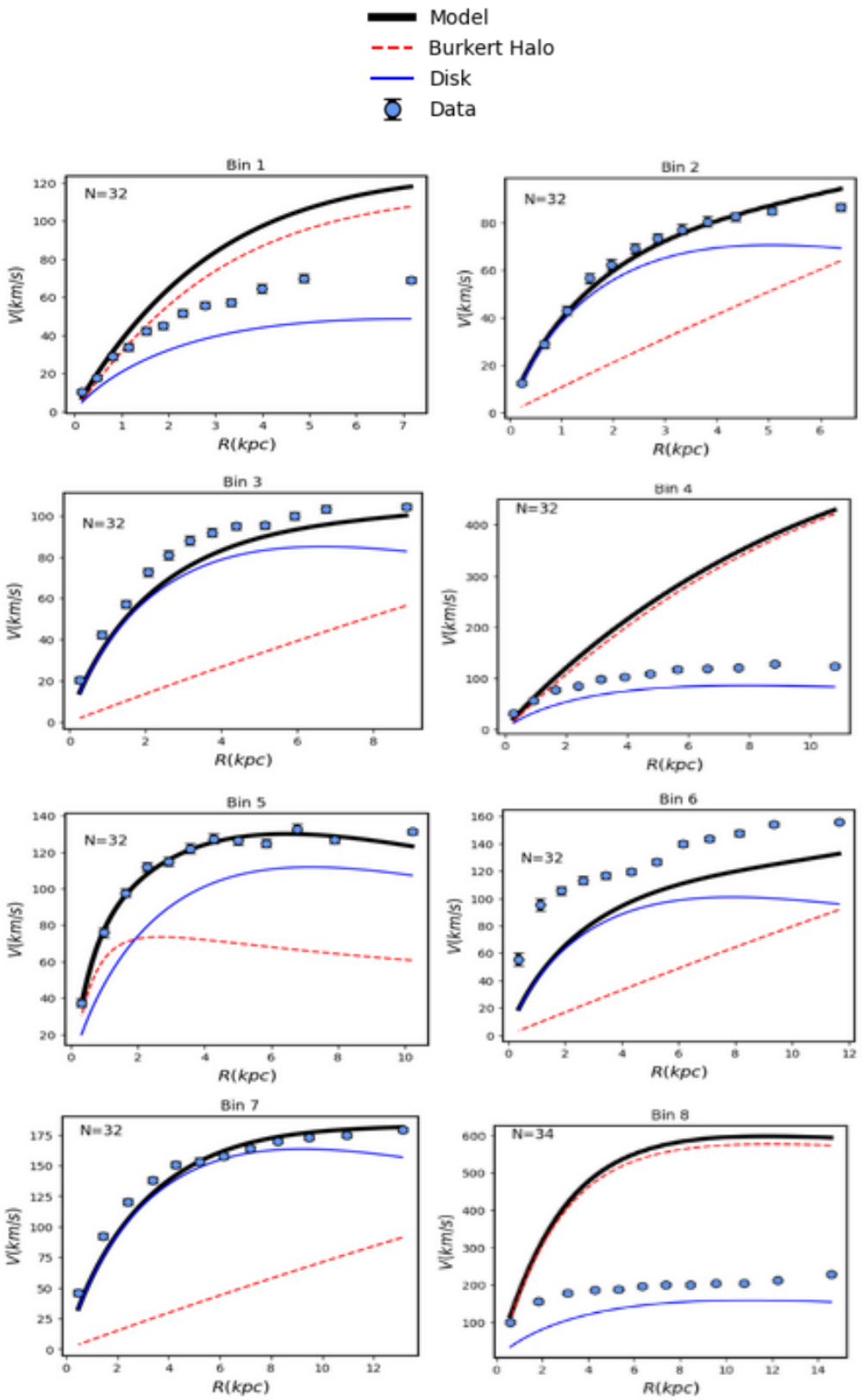

Figure 4.2: Fits for Burkert Halo

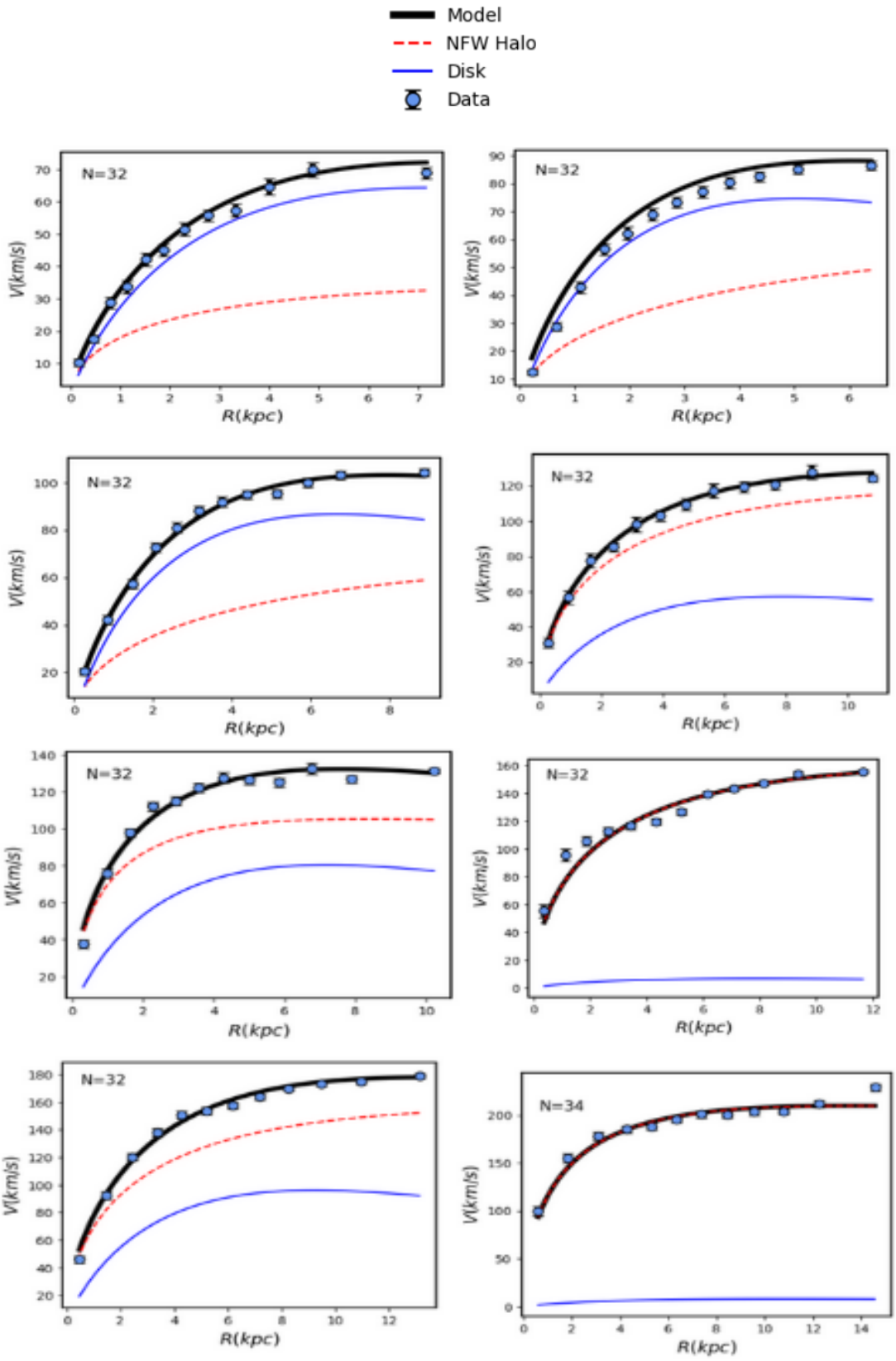

Figure 4.3: Fits for NFW Halo

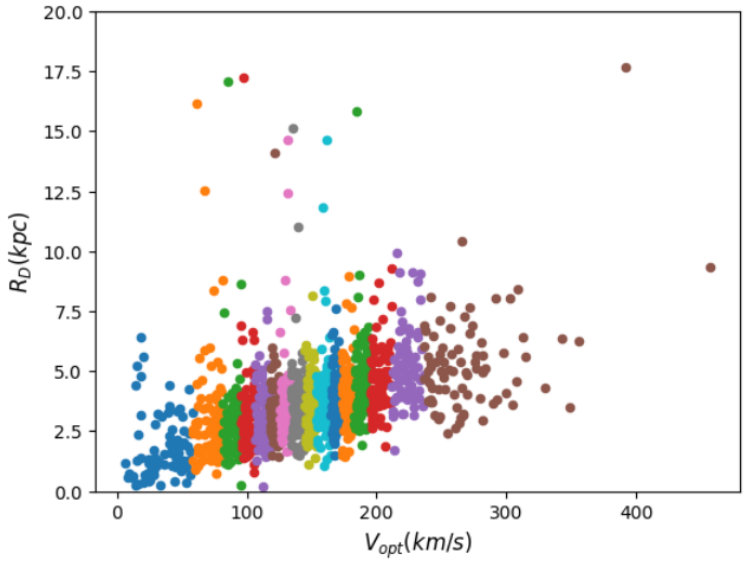

Figure 4.4: Bin-wise distribution of R_D in a larger sample of 1280 galaxies, after excluding 9 outliers with $R_D > 20$

	R_D, avg	V_{opt}
0	3.330025	53.113435
1	2.347514	82.968529
2	3.103892	99.752933
3	3.674343	115.851980
4	3.347863	133.262611
5	3.669161	153.623423
6	4.291618	179.670326
7	5.109350	240.853690

Figure 4.5: $< R_D >, < V_{opt} >$ in bins

PROBES Dataset is much more than expected. The values of $< R_D >$ in each bin are much larger than expected. For instance, the length scale of a large disk like Milky Way is 2.8 ± 0.3 kpc, which is smaller than the mean R_D of galaxies in the first bin. Our values are more similar to LSBs (Low Surface Brightness Galaxies) which normally have such large values of R_D(26). We tested our claim by drawing a larger sample from PROBES(of size 1280) but continued to face the same issue. Also note that, one would, in general, expect $< V_{opt} >$ to approximately increase with $< R_D >$ in each bin. This is not the case here, as seen in the following table. We changed the number of bins multiple times in order to verify this, however it appears that the PROBES Dataset has a problem with the values of R_D. And since this is a crucial quantity in MCMC fitting, we are not able to achieve a reasonable optimized set of parameters.

Chapter 5

Summary

In this project we attempted to model the rotation curves of spiral galaxies in the recent PROBES Dataset by separating their profiles into dark matter and baryonic contributions. We started by binning the RCs into bins of optical velocity, then radially, normalising them w.r.t R_{opt} and V_{opt} and finally coadding them so that systematic effects are minimized. Then we prepared synthetic rotation curves by denormalising them.
Dark Matter Contribution was modelled using both a Burkert(core) and NFW(cusp) profile. Baryonic contribution was limited to the consideration of the dominant disk component. We fit the model using an MCMC Code and found two key problems with the resulting fit: (i) In most cases, the velocity at larger radii was overestimated as compared to the observations, (ii) the disk component dominated the dark component at even large radii for several fits rendering our results wrong.
We tested our claim by increasing sample size, changing binning technique and changing the priors to see if they were wrong in the first place. After all this we zeroed in on the conclusion that the values of R_{opt} provided by the PROBES Dataset were much too large. Given that R_D is an important quantity for fitting, we were unsuccessful in obtaining reasonable results.

5.1 Appendix

5.1.1 Posterior Distribution Plots

Burkert Halo

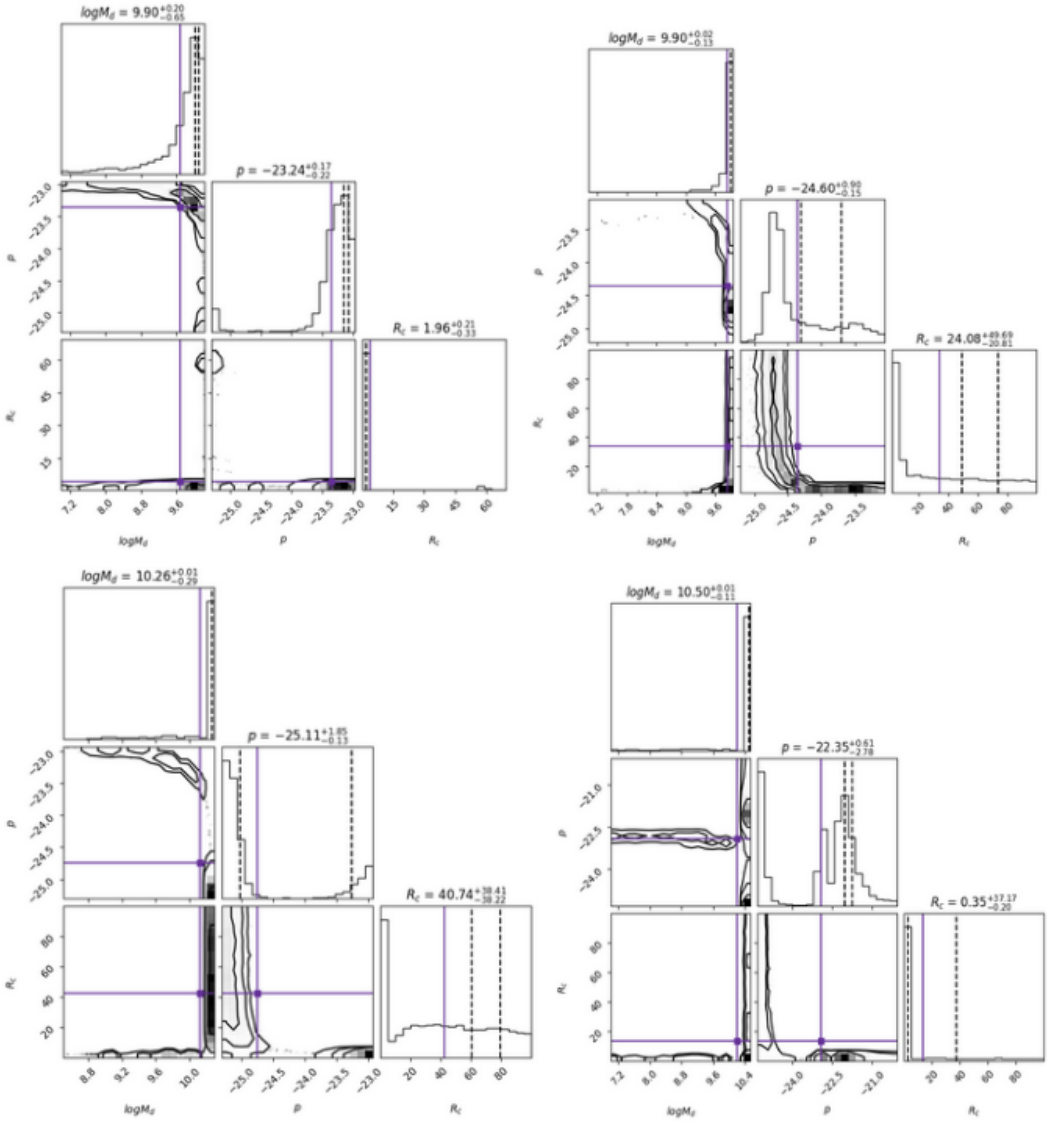

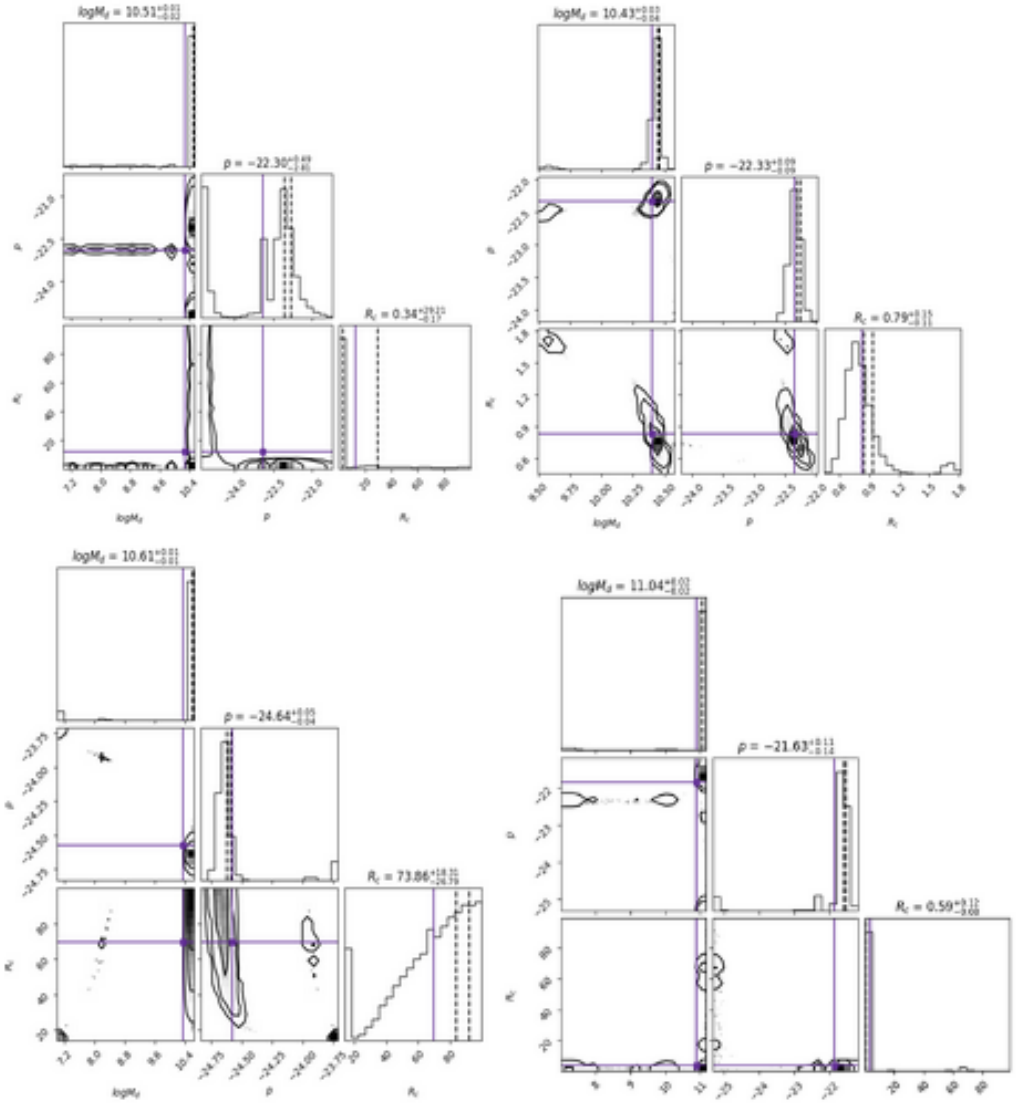

NFW Halo

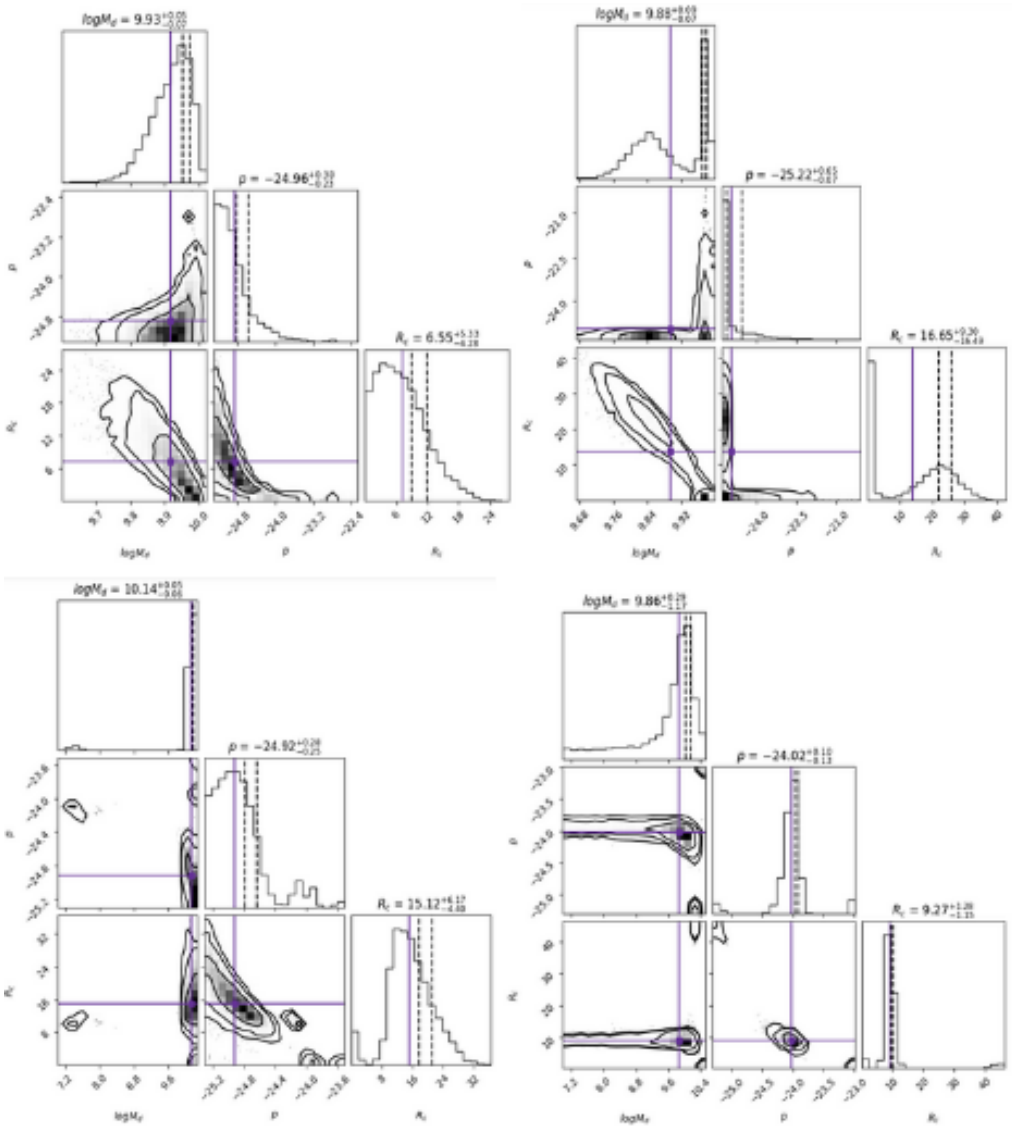

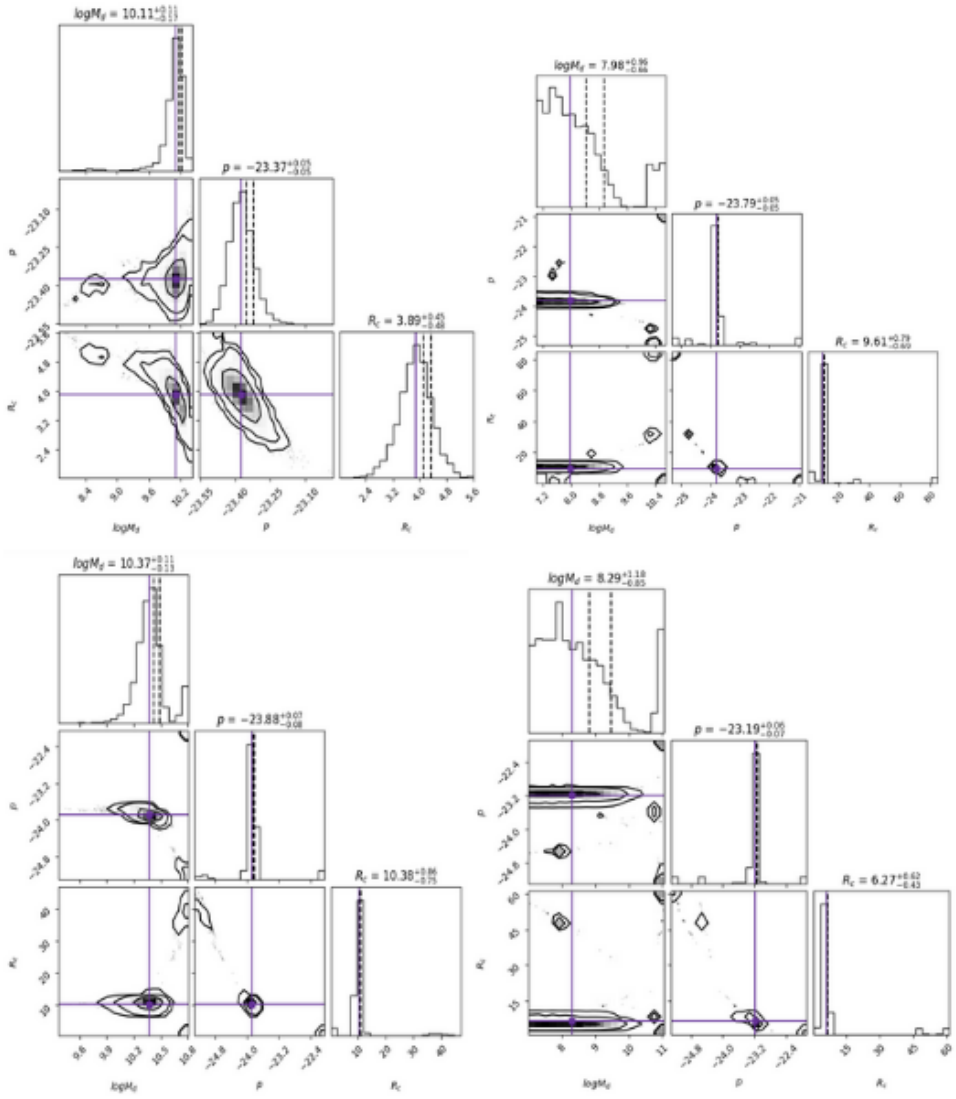

Chapter 6

Update on TNG Project

As an addendum to this work we state a couple of updates to a previous project. To remind the reader, the aim of this project was to leverage observational results to extract disk galaxies in the IllustrisTNG Simulation.

6.0.1 Recap

We had tried to filter galaxies based on their alignment with two empirical relations: the Star-Forming Main Sequence (SFMS)-between the log of Star Formation Rate(SFR) and the log of stellar mass($logM_\star$),and the Mass- Size Relation ($logR_{eff}$ vs $logM_\star$) with regards to the permitted scatter. We had used multiple versions of the Main Sequence Relation across redshifts to do so.

Close to the end of the project we had also suggested potential loopholes and a couple of methods to refine our analysis. For more details we refer the reader to `https://github.com/ambicagovind31/IllustrisTNG_Disks`, the repository where the previous report is uploaded.

The following paragraphs highlight the modifications made to this project with respect to the previous analysis.

6.0.2 Modifications

1. Given that observational results are afflicted by systematics and simulations are not, the use of magnitude of intrinsic scatter for $\sigma-$clipping is not the correct approach. One should use the total scatter which takes into account these observational results. This change was made.

2. The definitions of properties such as $M_\star$(stellar mass), SFR(Star Formation Rate) and R_{eff}(Effective Radius) can be very subjective. For example, TNG has three definitions of Subhalo Mass:

    - SubhaloMass: Total mass of all member particle/cells which are bound to this Subhalo, of all types.

- SubhaloMassInMaxRad: Sum of masses of all particles/cells within the radius of V_{max}(the maximum velocity attained in the spherically averaged galaxy rotation curve)
- SubhaloMassInRad: Sum of masses of all particles/cells within twice the stellar half mass radius.

Furthermore, R_{eff} in TNG is defined as the Subhalo Half Mass Radius, not the Stellar Half Mass Radius. A slight inconsistency in these fiducial definitions could affect the accuracy of the results, ever so little.
For R_{eff} we stuck to the earlier choice of Stellar Half Mass Radius, similar to other papers on TNG. We made all other choices consistent, such as masses and SFRs being those estimated at $2R_{eff}$, something which should have actually been done in the first place.

6.0.3 Resolutions

We also address three issues that we brought up as potential problems in our previous analysis:

(a) **The Main Sequence Turnover**: This was the discrepancy between several observational results wherein some observed a linear SFMS and some observed a flattening of slope close to the high mass end. It appears that the Main Sequence Turnover is at least partially result of selection effects, particularly color-color selection(27). Additionally, Johnston et al(28) showed that if one applies stricter cuts for what an SFG is, we end up with a linear SFMS, and with looser criteria a turnover appears. Thus, a linear SFMS will most likely have a larger percentage of disks. In that sense this turnover is not a significant issue and the choice of a linear relation would improve results.

(b) **Calibration and Standardization**: Since we need a compromise between calibration effects and the fact that relations specific to a redshift range will give better results for that bin, the results are to be done in both ways: by considering one equation applicable to the entire redshift range (29) and by considering separate relations within each bin and deciding the best fitting relation by eye. The latter may not logically be the most obvious way, but it would still solve the original purpose of extracting disks accurately.

(c) **Binning Issues**: Snapshots in TNG(which are datasets corresponding to each redshift), are organised into 20 full and 80 mini snapshots. The former has particle data of all kind, whereas the latter doesn't. Last time we had included only the full snapshots, but this time we included all of them irrespective of whether we have complete data available for the particles. This solved the problem of empty redshift bins, although the final dataset now needs to be filtered according to the data needed for analysis.

6.0.4 Yet Another Problem

One potential matter that I found with this approach which we avoid for now according to my guide's discretion is described as follows. A couple of newer papers on the Star Forming Main Sequence such as (30) state a quantitative discrepancy between results of observation and simulation. This is not surprising given the quality of fits obtained in the results even after the modifications(see samples below):

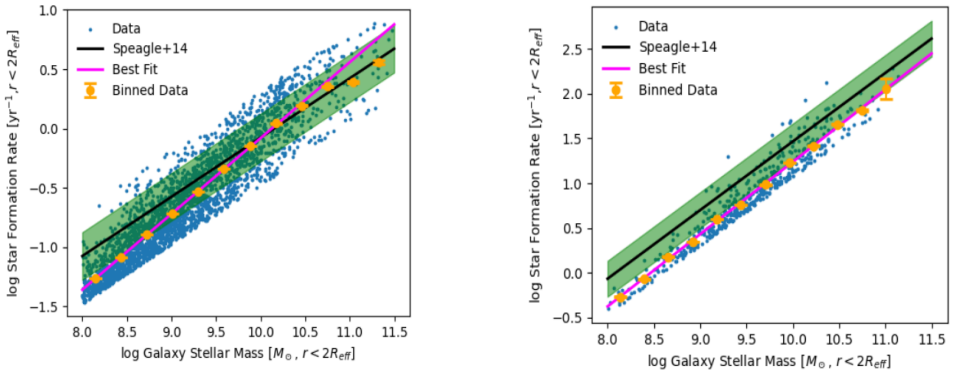

Figure 6.1: Best Fits on the Main Sequence for two snapshots obtained after 2σ clipping of TNG Data appear to be significantly offset w.r.t Speagle's Relation.

This problem is definitely reduced if we consider a different relation for each redshift range. Another way to possibly see the effects would be to apply one single relation of the $SFMS(z,t)$ at median redshift z to all the redshifts within a bin. This can,in principle, be done, but would require an unreasonably high computer memory. For example, the snapshot 99 corresponding to z=0 alone bears 1013.7 GB worth data. Therefore, a more prudent way is to load the data chunk by chunk and analyze each chunk sequentially.

In this case, it might be inaccurate to entirely depend on observational results to sieve disks. A better approach would be to extract disks in TNG independently, by binning and running median estimates of SFR and then check the images of a random sample to confirm the structure. In fact, this approach was taken in one of the first TNG papers(31). Note that newer studies are able to quell this discrepancy(32) by employing stronger Bayesian Inference algorithms to constrain observational results. If we do take the approach of leveraging observational results, we should probably use results such as these instead of old results as in Speagle's paper. Also note that if any of this fails, we can always resort to other criteria for selecting disks such as disk-to-spheroid ratio, and the growth of stellar mass within a timescale of the order of a Hubble time. For more details see (33).

Let it be known to the reader that simple tests to verify the disk-like nature of the drawn galaxies will be carried out again on these results once the method is approved. However, to be sure that the resultant disk sample is complete, its

more important to include maximum true positives than to exclude maximum false negatives- in essence, we not only need the resultant disks to be *just disks*, but also for them to span maximum disks in the simulation. This is why the extraction method carries a lot of importance.

We conclude this section by stating that we have made significant progress in our understanding of the simulation landscape. A more thorough literature review has also been performed. More changes will be made in the future based on the suggestions of the guide.

Data Availability

All codes and data used in this project can be found on this GitHub Repository: `https://github.com/ambicagovind31/RC-Modelling`. Updated codes and results for the TNG Project are available here in the file Disks Speagle.zip: `https://github.com/ambicagovind31/IllustrisTNG_Disks`

Bibliography

[1] A. Bosma, "arxiv e-prints arxiv:2309.06390 (2023)," 2023. pages 1

[2] F. Zwicky, "Helvetica physica acta, 6, 110," 1933. pages 1

[3] S. Giodini, D. Pierini, A. Finoguenov, G. W. Pratt, H. Boehringer, A. Leauthaud, L. Guzzo, H. Aussel, M. Bolzonella, P. Capak, M. Elvis, G. Hasinger, O. Ilbert, J. S. Kartaltepe, A. M. Koekemoer, S. J. Lilly, R. Massey, H. J. McCracken, J. Rhodes, M. Salvato, D. B. Sanders, N. Z. Scoville, S. Sasaki, V. Smolcic, Y. Taniguchi, and D. Thompson, "Stellar and total baryon mass fractions in groups and clusters since redshift 1*," *The Astrophysical Journal*, vol. 703, p. 982–993, Sept. 2009. pages 1

[4] V. C. Rubin, W. K. Ford Jr, and N. Thonnard, "Extended rotation curves of high-luminosity spiral galaxies. iv-systematic dynamical properties, sa through sc," *Astrophysical Journal, Part 2-Letters to the Editor, vol. 225, Nov. 1, 1978, p. L107-L111.*, vol. 225, pp. L107–L111, 1978. pages 2

[5] H. W. Babcock, "The rotation of the andromeda nebula," *Lick Observatory bulletin; no. 498; Lick Observatory bulletins; no. 498., Berkeley: University of California Press,[1939], p. 41-51,[2] leaves of plates; 31 cm.*, vol. 19, pp. 41–51, 1939. pages 2

[6] A. Bosma, "21-cm line studies of spiral galaxies. i-observations of the galaxies ngc 5033, 3198, 5055, 2841, and 7331," *Astronomical Journal, vol. 86, Dec. 1981, p. 1791-1824. Research supported by the Nederlandse Organisatie voor Zuiver-Wetenschappelijk Onderzoek*, vol. 86, pp. 1791–1824, 1981. pages 2

[7] E. Corbelli and P. Salucci, "The extended rotation curve and the dark matter halo of m33," *Monthly Notices of the Royal Astronomical Society*, vol. 311, p. 441–447, Jan. 2000. pages 2

[8] N. Aghanim, Y. Akrami, M. Ashdown, J. Aumont, C. Baccigalupi, M. Ballardini, A. J. Banday, R. B. Barreiro, N. Bartolo, S. Basak, R. Battye, K. Benabed, J.-P. Bernard, M. Bersanelli, P. Bielewicz, J. J. Bock, J. R. Bond, J. Borrill, F. R. Bouchet, F. Boulanger, M. Bucher, C. Burigana, R. C. Butler, E. Calabrese, J.-F. Cardoso, J. Carron, A. Challinor, H. C. Chiang, J. Chluba, L. P. L. Colombo, C. Combet, D. Contreras, B. P. Crill,

F. Cuttaia, P. de Bernardis, G. de Zotti, J. Delabrouille, J.-M. Delouis, E. Di Valentino, J. M. Diego, O. Doré, M. Douspis, A. Ducout, X. Dupac, S. Dusini, G. Efstathiou, F. Elsner, T. A. Enßlin, H. K. Eriksen, Y. Fantaye, M. Farhang, J. Fergusson, R. Fernandez-Cobos, F. Finelli, F. Forastieri, M. Frailis, A. A. Fraisse, E. Franceschi, A. Frolov, S. Galeotta, S. Galli, K. Ganga, R. T. Génova-Santos, M. Gerbino, T. Ghosh, J. González-Nuevo, K. M. Górski, S. Gratton, A. Gruppuso, J. E. Gudmundsson, J. Hamann, W. Handley, F. K. Hansen, D. Herranz, S. R. Hildebrandt, E. Hivon, Z. Huang, A. H. Jaffe, W. C. Jones, A. Karakci, E. Keihänen, R. Keskitalo, K. Kiiveri, J. Kim, T. S. Kisner, L. Knox, N. Krachmalnicoff, M. Kunz, H. Kurki-Suonio, G. Lagache, J.-M. Lamarre, A. Lasenby, M. Lattanzi, C. R. Lawrence, M. Le Jeune, P. Lemos, J. Lesgourgues, F. Levrier, A. Lewis, M. Liguori, P. B. Lilje, M. Lilley, V. Lindholm, M. López-Caniego, P. M. Lubin, Y.-Z. Ma, J. F. Macías-Pérez, G. Maggio, D. Maino, N. Mandolesi, A. Mangilli, A. Marcos-Caballero, M. Maris, P. G. Martin, M. Martinelli, E. Martínez-González, S. Matarrese, N. Mauri, J. D. McEwen, P. R. Meinhold, A. Melchiorri, A. Mennella, M. Migliaccio, M. Millea, S. Mitra, M.-A. Miville-Deschênes, D. Molinari, L. Montier, G. Morgante, A. Moss, P. Natoli, H. U. Nørgaard-Nielsen, L. Pagano, D. Paoletti, B. Partridge, G. Patanchon, H. V. Peiris, F. Perrotta, V. Pettorino, F. Piacentini, L. Polastri, G. Polenta, J.-L. Puget, J. P. Rachen, M. Reinecke, M. Remazeilles, A. Renzi, G. Rocha, C. Rosset, G. Roudier, J. A. Rubiño-Martín, B. Ruiz-Granados, L. Salvati, M. Sandri, M. Savelainen, D. Scott, E. P. S. Shellard, C. Sirignano, G. Sirri, L. D. Spencer, R. Sunyaev, A.-S. Suur-Uski, J. A. Tauber, D. Tavagnacco, M. Tenti, L. Toffolatti, M. Tomasi, T. Trombetti, L. Valenziano, J. Valiviita, B. Van Tent, L. Vibert, P. Vielva, F. Villa, N. Vittorio, B. D. Wandelt, I. K. Wehus, M. White, S. D. M. White, A. Zacchei, and A. Zonca, "Planck2018 results: Vi. cosmological parameters," *Astronomy amp; Astrophysics*, vol. 641, p. A6, Sept. 2020. pages 2

[9] C. J. Copi, D. N. Schramm, and M. S. Turner, "Big-bang nucleosynthesis and the baryon density of the universe," *Science*, vol. 267, p. 192–199, Jan. 1995. pages 2

[10] P. A. R. Ade, N. Aghanim, M. Arnaud, M. Ashdown, and A. et al, "Planck2015 results: Xiii. cosmological parameters," *Astronomy amp; Astrophysics*, vol. 594, p. A13, Sept. 2016. pages 2

[11] R. Massey, T. Kitching, and J. Richard, "The dark matter of gravitational lensing," *Reports on Progress in Physics*, vol. 73, p. 086901, July 2010. pages 2

[12] B. Ratra and M. S. Vogeley, "The beginning and evolution of the universe," *Publications of the Astronomical Society of the Pacific*, vol. 120, no. 865, p. 235, 2008. pages 3, 4

[13] B. Famaey and S. S. McGaugh, "Modified newtonian dynamics (mond):

Observational phenomenology and relativistic extensions," *Living Reviews in Relativity*, vol. 15, Sept. 2012. pages 3

[14] S. Cebrián, "Review on dark matter searches," *Journal of Physics: Conference Series*, vol. 2502, p. 012004, May 2023. pages 3

[15] T. M. Undagoitia and L. Rauch, "Dark matter direct-detection experiments," *Journal of Physics G: Nuclear and Particle Physics*, vol. 43, p. 013001, Dec. 2015. pages 3

[16] J. P. Ostriker and P. J. Peebles, "A numerical study of the stability of flattened galaxies: or, can cold galaxies survive?," *Astrophysical Journal, Vol. 186, pp. 467-480 (1973)*, vol. 186, pp. 467–480, 1973. pages 3

[17] M. Persic and P. Salucci, "Dark and visible matter in spiral galaxies," *Monthly Notices of the Royal Astronomical Society*, vol. 234, no. 1, pp. 131–154, 1988. pages 3

[18] G. de Vaucouleurs, "Recherches sur les nebuleuses extragalactiques," *Annales d'Astrophysique, Vol. 11, p. 247*, vol. 11, p. 247, 1948. pages 4

[19] K. C. Freeman, "On the disks of spiral and s0 galaxies," *Astrophysical Journal, vol. 160, p. 811*, vol. 160, p. 811, 1970. pages 4

[20] J. F. Navarro, C. S. Frenk, and S. D. White, "A universal density profile from hierarchical clustering," *The Astrophysical Journal*, vol. 490, no. 2, p. 493, 1997. pages 4

[21] J. Einasto, "On the construction of a composite model for the galaxy and on the determination of the system of galactic parameters," *Trudy Astrofizicheskogo Instituta Alma-Ata, Vol. 5, p. 87-100, 1965*, vol. 5, pp. 87–100, 1965. pages 4

[22] L. Chemin, W. J. G. de Blok, and G. A. Mamon, "Improved modeling of the mass distribution of disk galaxies by the einasto halo model," *The Astronomical Journal*, vol. 142, p. 109, Aug. 2011. pages 4

[23] A. Burkert, "The structure of dark matter halos in dwarf galaxies," *The Astrophysical Journal*, vol. 447, no. 1, p. L25, 1995. pages 4

[24] C. Stone, S. Courteau, N. Arora, M. Frosst, and T. H. Jarrett, "Probes. i. a compendium of deep rotation curves and matched multiband photometry," *The Astrophysical Journal Supplement Series*, vol. 262, p. 33, Sept. 2022. pages 7

[25] D. Foreman-Mackey, D. W. Hogg, D. Lang, and J. Goodman, "emcee: the mcmc hammer," *Publications of the Astronomical Society of the Pacific*, vol. 125, no. 925, p. 306, 2013. pages 14

[26] C. Di Paolo, P. Salucci, and A. Erkurt, "The universal rotation curve of low surface brightness galaxies – IV. The interrelation between dark and luminous matter," *Mon. Not. Roy. Astron. Soc.*, vol. 490, no. 4, pp. 5451–5477, 2019. pages 18

[27] W. J. Pearson, F. Pistis, M. Figueira, K. Małek, T. Moutard, D. Vergani, and A. Pollo, "Influence of star-forming galaxy selection on the galaxy main sequence," *Astronomy amp; Astrophysics*, vol. 679, p. A35, Oct. 2023. pages 25

[28] R. Johnston, M. Vaccari, M. Jarvis, M. Smith, E. Giovannoli, B. Häußler, and M. Prescott, "The evolving relation between star formation rate and stellar mass in the video survey sincez = 3," *Monthly Notices of the Royal Astronomical Society*, vol. 453, p. 2541–2558, Aug. 2015. pages 25

[29] J. S. Speagle, C. L. Steinhardt, P. L. Capak, and J. D. Silverman, "A highly consistent framework for the evolution of the star-forming "main sequence" from z 0-6," *The Astrophysical Journal Supplement Series*, vol. 214, p. 15, Sept. 2014. pages 25

[30] P. Popesso, A. Concas, G. Cresci, S. Belli, G. Rodighiero, H. Inami, M. Dickinson, O. Ilbert, M. Pannella, and D. Elbaz, "The main sequence of star-forming galaxies across cosmic times," *Monthly Notices of the Royal Astronomical Society*, vol. 519, p. 1526–1544, Nov. 2022. pages 26

[31] M. Donnari, A. Pillepich, D. Nelson, M. Vogelsberger, S. Genel, R. Weinberger, F. Marinacci, V. Springel, and L. Hernquist, "The star formation activity of illustristng galaxies: main sequence, uvj diagram, quenched fractions, and systematics," *Monthly Notices of the Royal Astronomical Society*, vol. 485, p. 4817–4840, Mar. 2019. pages 26

[32] E. J. Nelson, S. Tacchella, B. Diemer, J. Leja, L. Hernquist, K. E. Whitaker, R. Weinberger, A. Pillepich, D. Nelson, B. A. Terrazas, R. Nevin, G. B. Brammer, B. Burkhart, R. K. Cochrane, P. van Dokkum, B. D. Johnson, F. Marinacci, L. Mowla, R. Pakmor, R. E. Skelton, J. Speagle, V. Springel, P. Torrey, M. Vogelsberger, and S. Wuyts, "Spatially resolved star formation and inside-out quenching in the tng50 simulation and 3d-hst observations," *Monthly Notices of the Royal Astronomical Society*, vol. 508, p. 219–235, Aug. 2021. pages 26

[33] S. Tacchella, B. Diemer, L. Hernquist, S. Genel, F. Marinacci, D. Nelson, A. Pillepich, V. Rodriguez-Gomez, L. V. Sales, V. Springel, and M. Vogelsberger, "Morphology and star formation in illustristng: the build-up of spheroids and discs," *Monthly Notices of the Royal Astronomical Society*, vol. 487, p. 5416–5440, June 2019. pages 26